Compact and Sharp-Rejection Bandstop Filter Using Uniplanar Double Spiral Resonant Cells

Ke LU, Guang-Ming WANG, He-Xiu XU

Missile Institute of Air Force Engineering University, Sanyuan, Shaanxi, 713800, China

lookluna@126.com, wgming01@sina.com, hxxu2008@yahoo.cn

Abstract. *A novel compact bandstop filter composed of three cascaded uniplanar double spiral resonant cells (UDSRCs) for high attenuation rates is presented. Through the equivalent circuit prediction and parametric analysis, it is found that the UDSRC exhibits two controllable transmission zeros with great design flexibility through tuning the geometry parameters in a small range. Then, the influence of the stage separation between each UDSRC is investigated in order to get the appropriate stage separation. After optimization, a demonstration bandstop filter has been fabricated and measured. The results show that the attenuation rates on the lower and upper sides are 95 dB/GHz and 155 dB/GHz, respectively. Without any shunt stubs introduced, the length and width of the three cells are 28% and 4% of the guided wavelength at the mid-stopband frequency.*

Keywords

Uniplanar double spiral resonant cell, controllable transmission zeros, compact size, high attenuation rates.

1. Introduction

Microstrip bandstop filters are widely utilized to block interfered signals and suppress spurious harmonics because of easy fabrication and low weight. The bandstop filters utilizing shunt open-circuited stubs suffer from slow roll-off and comparatively large size. Alternatively, microstrip bandstop filters have been developed by utilizing the defected ground structure (DGS) [1], [2]. Whereas, there is a back radiation problem which is common for the DGS and additional metallic plane must be appropriately put underneath the ground of microstrip components at the cost of increased weight and inevitable complexity. Recently, signal interference technique was introduced to design wide stopband bandstop filters with high selectivity, but the given filters suffer from large dimension, especially the extended width [3], [4]. On the other hand, UDSRC was initially proposed in [5] and it was demonstrated that UDSRC printed on grounded dielectric substrate possesses left-handed propagation property throughout the Brillouin zone. The bandpass property of one dimensional transmission line composed of UDSRCs with gaps between each other has been proved [6]. Recently, UDSRC was applied in low-profile folded monopoles as the metamaterial phase-shifting line. In this letter, UDSRCs are applied to synthesis one compact and sharp-rejection bandstop filter. Through equivalent circuit prediction and parametric analysis, it is found that the UDSRC embedded in the microstrip line exhibits bandstop property with two controllable transmission zeros while the bandstop property can be optimized effectively through tuning the geometry parameters. Through cascading three different UDSRCs, satisfactory bandstop property around the designed mid-stopband frequency has been achieved. At the same time, the effect of the stage separation on the filter performance is investigated. It is demonstrated that the bandstop property is affected by too short stage separation due to the magnetic coupling between each UDSRC, but the short stage separation does not deteriorate the filter performance greatly. Without any DGSs or shunt stubs introduced, the total length of three cells and the width of the cells are about 31.2 mm ($0.28\lambda_g$) and 4.6 mm ($0.04\ \lambda_g$), respectively, where λ_g is the guided wavelength at the mid-stopband frequency. To the best of our knowledge, this is the narrowest filter so far reported in the literature. The proposed filter is very suitable for RF/microwave integrated circuit application.

2. Characterization of UDSRC

The layout of UDSRC embedded in the microstrip line is shown in Fig. 1. In the past, UDSRC was treated as half-wavelength resonator whose conducting wire was folded in the spiral pattern [7], but the complex electromagnetic coupling phenomenon resulted from its special structure must be considered and this factor may influence the characterization of UDSRC intensively. Thus, an equivalent circuit of UDSRC is proposed as shown in Fig. 2. C1 and L1 stand for the capacitance and inductance when UDSRC operates as a half-wavelength resonator. Cm is the capacitance which is utilized to model the displacement current between the adjacent conducting wires of the two single spirals [6] while Lm represents the mutual magnetic coupling between the two single spirals, which was neglected in the equivalent circuit of UDSRC proposed in

[6]. It is obvious that Cm and Lm can provide another transmission zero at their resonant frequency. To demonstrate the validity of the proposed equivalent circuit, the four circuit parameters are extracted using curve fitting procedure. Then, the simulated S21 from the proposed equivalent circuit and full-wave simulation are compared. In the full-wave simulation, the unit with L1 = 4.3 mm, W2 = 0.4 mm, W1 = 4.6 mm (equal to the width of microstrip 50ohm line), W3 = 0.4 mm and W4 = 0.2 mm was utilized. The substrate with relative dielectric constant of 2.2 and thickness of 1.5 mm was utilized in both simulation and fabrication. As shown in Fig. 2, a good agreement can be seen from 1 GHz to 5 GHz. Furthermore, as the proposed equivalent circuit predicts, there are two transmission zeros. Based on the above, the given circuit is usable and can provide the main operation principle of the proposed structure.

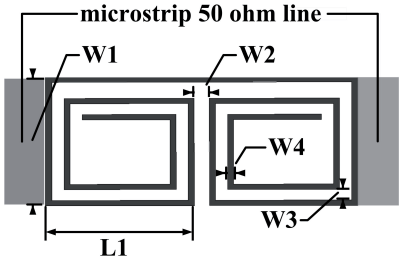

Fig. 1. Layout of UDSRC embedded in the microstrip line.

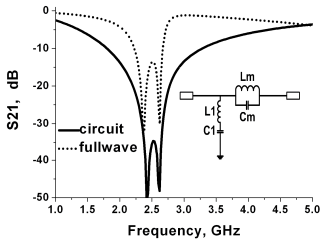

Fig. 2. Comparison of the simulated S21 of the proposed equivalent circuit and full-wave simulation. The extracted circuit parameters are: C1 = 0.16356 pF, Cm=0.354259 pF, L1=22.70499 nH, Lm=12.12310 nH

3. Effect of the Geometry Parameters

In order to investigate UDSRC further, parametric analysis of L1, W2, W3 and W4 should be implemented, respectively. Fig. 3 shows the effect of L1 on S21. As observed in Fig. 3, with the increase of L1, the two transmission zeros both shift to the lower frequency band. It is obvious that the variation of L1 can change the physical length of UDSRC significantly. Additionally, the zero separation approximately remains unchanged. Then, Fig. 4 shows the variation of S21 with W2. As shown in Fig. 4, the transmission zeros derived from the resonance when UDSRC operates as a half-wavelength resonator (which is donated as f1 in Fig. 4) change insignificantly with W2. This is because W2 has a comparatively small degree of control on the physical length of UDSRC. Further, the transmission zero resulted from the resonance of Cm and Lm (which is donated as f2 in Fig. 4) shifts to the higher frequency band with the increase of W2. As referred in [8], the electric coupling and the magnetic coupling both decay against the spacing. So, with the increase of W2, the electric coupling and magnetic coupling both degenerate. Namely, the values of Lm and Cm both become small which lead to the increase of f2. This conclusion agrees well with the full-wave simulated results and the validity of the equivalent circuit is demonstrated once again. In addition, the parametric analysis of W3 and W4 is implemented and the given results are shown in Fig. 5 and Fig. 6, respectively. As depicted in Fig. 5, it can be seen that the stopband shifts upwards with the increase of W3. Simultaneously, as observed in Fig. 6, the increase of W4 will also make the stopband shift to the higher frequency band. Because the minimized fabrication tolerance which can be achieved in our limited conditions is 0.1 mm and the width of UDSRC is very narrow, the values of W3 and W4 which can be utilized is within quite limited range. So, L1 and W2 are choosed to be the primary adjustment parameters. W1 = 4.6 mm, W3 = 0.4 mm and W4 = 0.2 mm are kept constant throughout.

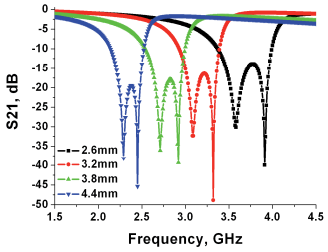

Fig. 3. Variation of the frequency response of the S21 with L1. W2 = 1 mm, W3 = 0.4 mm and W4 = 0.2 mm.

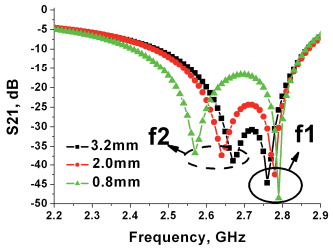

Fig. 4. Variation of the frequency response of the S21 with W2. Ll = 4 mm, W3 = 0.4 mm and W4 = 0.2 mm.

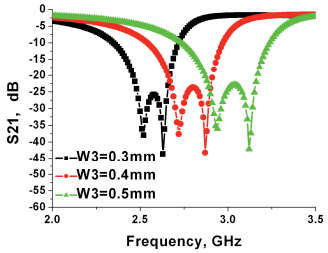

Fig. 5. Variation of the frequency response of the S21 with W3. L1 = 4.4 mm, W2 = 2 mm and W4 = 0.4 mm.

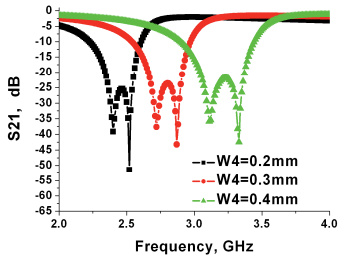

Fig. 6. Variation of the frequency response of the S21 with W4. L1 = 4.4 mm, W2 = 2 mm and W3 = 0.3 mm.

4. Design and Fabrication

Based on the above, the benefit of UDSRC is that it exhibits two controllable transmission zeros, which can enhance the rejection level or attenuation rates at the specified frequency. As shown in Fig. 7, three UDSRCs are cascaded to synthesis one bandstop filter whose mid-stopband frequency is designed to be 2.7 GHz. The cells are connected with two 50ohm lines with the length of d. Three UDSRCs can provide six transmission zeros which facilitate a wide control over the rejection level, attenuation rates and stopband width, simultaneously. The full-wave simulator HFSS has been utilized to obtain the optimized dimensions of the three units which are listed in Tab. 1. Additionally, because there is magnetic coupling between each UDSRC, the stage separation, d, will affect the bandstop property of the proposed filter. Thus, the S21 of individual UDSRCs utilized in the proposed filter are listed and compared with the proposed filter with different stage separations as shown in Fig. 8. It is demonstrated that the long stage separation can protect the magnetic coupling effectively while the short stage separation will lead to the result that the transmission zeros shift from the ones of the individual UDSRCs embedded in the microstrip line. As depicted in Fig. 8, the magnetic coupling is not necessary to protect because this phenomenon does not degenerate the bandstop property greatly. Whereas, this special feature may be utilized to broaden the stopband width as shown in Fig. 8. Moreover, the short stage separation will yield very compact total length of the proposed bandstop filter. Subsequently, the stage separation, d, is set to be 1 mm. To facilitate soldering, two 12 mm long 50ohm lines have been cascaded at the input and output ports. Photograph of the fabricated prototype is shown in Fig. 9. The prototype was measured using an Anritsu ME7808A vector network analyzer while the simulated and measured results are shown in Fig. 10. The measured stopband attenuation level is more than 20 dB approximately from 2.25 to 3.21 GHz. The attenuation rate on the lower side of the stopband is approximately 95 dB/GHz (S21 being -3 dB and -47.5 dB at 1.85 and 2.32 GHz, respectively) while the one on the upper side is about 155 dB/GHz (S21 being -3 dB and -30.9 dB at 3.35 and 3.17 GHz, respectively). The length of three cells is 31.2 mm ($0.28\lambda_g$) and the width of UDSRCs is 4.6 mm ($0.04\ \lambda_g$). λ_g is the guided wavelength at the mid-stopband frequency, 2.73 GHz.

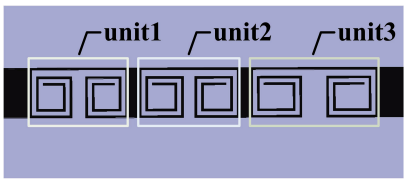

Fig. 7. Layout of the proposed bandstop filter.

	unit 1	unit 2	unit 3
L1 [mm]	3.8	4	4.6
W2 [mm]	1.2	1	2.2

Tab. 1. Summary of the geometry parameters of the three cells.

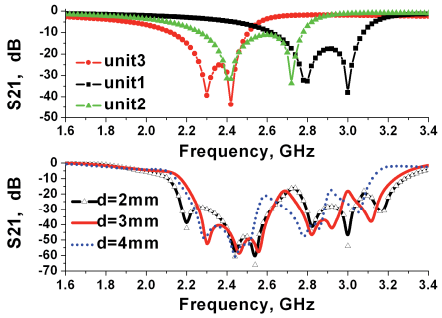

Fig. 8. S21 of the individual UDSRCs embedded in the microstrip line and the ones of the proposed filter with different stage separation.

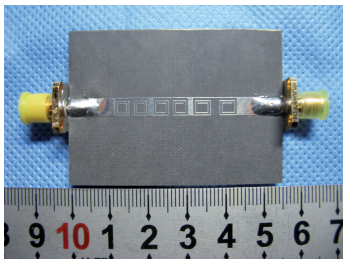

Fig. 9. Photograph of the proposed bandstop filter.

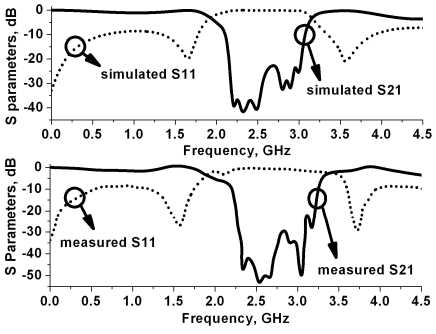

Fig. 10. Simulated and measured results of the bandstop filter.

5. Conclusion

In this letter, one bandstop filter composed of three cascaded UDSRCs is proposed. The UDSRC exhibits two controllable transmission zeros which can be adjusted through tuning the geometry parameters. Through optimizing the dimensions of the three cells and choosing the appropriate stage separation, enhanced rejection level, wide

stopband and high attenuation rates have been achieved. What is more, the size of the proposed filter is very compact and no shunt stub or defected ground structure is introduced. The proposed filter has the potential of applying to RF/microwave integrated circuits.

Acknowledgements

This work is supported by the National Natural Science Foundation of China under Grant Nos. 60971118. The authors would also like to thank the China North Electronic Engineering Research Institute for the fabrication.

References

[1] DUK-JAE, W., TAEK-KYUNG, L., JAE-WOOK, L., CHEOL-SIG, P., WON-KYU, C. Novel U-slot and V-slot DGSs for bandstop filter with improved Q factor. *IEEE Transactions on Microwave Theory and Techniques,* June, 2006, vol. 54, no. 6, p. 2840 – 2847.

[2] IAO-HUA, W., BING-ZHONG, W., HUA-LIANG, Z., KEVIN, J.C. A tunable bandstop resonator based on a compact slotted ground structure, *IEEE Transactions on Microwave Theory and Techniques*, September, 2007, vol. 55, no. 9, p. 1912 – 918.

[3] MANDAL, M. K., MONDAL, P., Design of sharp-rejection, compact, wideband, bandstop filters. *IET Microwaves, Antennas & Propagation*, 2008, vol. 2, no. 4, p. 389 – 393.

[4] KRISHNA VELIDI, V., BABU GUNTUPALLI, A., SUBRATA, S. Sharp-rejection ultra-wide bandstop filters. I*EEE Microwave and Wireless Component Letter*, 2009, vol. 19, no. 8, p. 503 – 505.

[5] YUNCHUAN, G., GOUSSETIS, G., FERESIDIS, A. P., VARDAXOGLOU, J. C. Efficient modeling of novel uniplanar left-handed metamaterials. *IEEE Transactions on Microwave Theory and Techniques*, 2005, vol. 53, no. 4, p. 1462 – 1468.

[6] KOKKINOS, T., FERESIDIS, A. P., VARDAXOGLOU, J. C. Equivalent circuit of double spiral resonators supporting backward waves. In *Loughborough Antennas and Propagation Conference.* Loughborough (UK), 2007, p. 289 – 292.

[7] KOKKINOS, T., FERESIDIS, A. P. Low-profile folded monopoles with embedded planar metamaterial phase-shifting lines. *IEEE Transactions on Antennas and Propagatio*n, 2009, vol. 57, no. 10, p. 2997 – 3008.

[8] JIA-SHENG, H., LANCASTER, M. J. *Microstrip Filters for RF/Microwave Applications*. New York: Wiley, 2001.

About Authors...

Ke LU was born in Shanxi province of China. He received the B.S. degree in Electrical Engineering and M.S. degree in the Communication and Information Systems in 2006 and 2009, respectively, from the Air Force Engineering University, where he is currently working toward the Ph.D. degree. His research interests include the design and applications of metamaterials.

Guang-Ming WANG was born in Anhui province of China. He received his B.S. and M.S. degrees from the Missile Institute of Air Force Engineering University, Xi'an, China, in 1982 and 1990, respectively, and his Ph.D. degree from the Electronic Science and Technology University, Chengdu, China, in 1994. Then, he joined the Air Force Engineering University as a professor in 2000 and is now the head of the Microwave Laboratory center in it. His current interest includes microwave circuits, antenna and propagation, and also the new structures include EBG, PBG, metamaterials and fractals, etc.

He-Xiu XU was born in the Jiangxi province of China. He received his B.S. degree in Communication Engineering from the Missile Institute of Air Force Engineering University, Xi'an, China, in 2008. His research interests include metamaterials and fractals geometry.